

BROADBAND MEASUREMENTS OF FACULAR PHOTOMETRIC CONTRAST USING THE SOLAR BOLOMETRIC IMAGER

PETER FOUKAL

Heliophysics, Inc., 192 Willow Road, Nahant, MA 01908; pfoukal@world.std.com

AND

PIETRO BERNASCONI, HARRY EATON, AND DAVID RUST

Johns Hopkins University Applied Physics Laboratory, 1110 Johns Hopkins Road, Laurel, MD 20723;

pietro.bernasconi@jhuapl.edu, harry.eaton@jhuapl.edu, david.rust@jhuapl.edu

Received 2004 May 25; accepted 2004 June 29; published 2004 July 13

ABSTRACT

We present the first photometric measurements of solar faculae *in broadband light*. Our measurements were made during the recent flight of the Solar Bolometric Imager (SBI), a 30 cm balloon-borne telescope that imaged the Sun with a spectrally constant response between about 0.31 and 2.6 μm . Our curve of facular contrast versus limb distance agrees well with values obtained by the blackbody correction of monochromatic measurements. This decreases uncertainty in the facular irradiance contribution, which limits searches for other possible mechanisms of solar luminosity variation, besides changes of photospheric magnetism.

Subject headings: solar-terrestrial relations — Sun: activity — Sun: faculae, plages — Sun: magnetic fields — Sun: photosphere

1. INTRODUCTION

Empirical models demonstrate a high correlation between fluctuations of total solar irradiance, S , and area variations of photospheric magnetic structures: sunspots, faculae, and the enhanced network (e.g., Willson et al. 1981; Foukal & Lean 1988; Krivova et al. 2003). The correlation found indicates that over 80% of the variance is *proportional* to the competing influences of bright and dark photospheric magnetic structures. But the correspondence in *amplitude* is much less certain. The reason is that, while the wideband photometric contrasts for spots are relatively well measured, the more fragmented faculae and enhanced network are more difficult to observe (e.g., Lawrence 1988; Lawrence et al. 1993). Consequently, the models mainly rely on proxies, such as the microwave index F10.7, or the Mg II line/continuum ratio (e.g., Foukal & Lean 1986; Chapman et al. 1996). Models based on actual estimates of the facular broadband contrast (e.g., Foukal et al. 1991; Lean et al. 1998; Fligge et al. 1998) are insufficiently accurate to determine how closely the modeled and radiometrically observed fluctuations correspond in amplitude.

This comparison in amplitude is required to determine whether the rotational and 11 yr modulation of total irradiance is accounted for entirely by dark spots and bright faculae or whether other, slower variations of solar luminosity might exist to drive climate (e.g., Foukal 2003). We describe here the first broadband photometric observations suitable for measurement of the facular contribution to variation in S with an accuracy comparable to that achieved in the space-borne radiometry.

2. INSTRUMENTATION

The most accurate measurement of the broadband photometric contribution of photospheric magnetic structures would be provided by an optical system having wideband, nonselective spectral response similar to a space-borne radiometer such as the Active Cavity Radiometer Irradiance Monitor (ACRIM). Such an instrument, the Solar Bolometric Imager (SBI), has recently been developed (Foukal & Libonate 2001; Bernasconi et al. 2004) and flown on a balloon (Bernasconi et al. 2003).

The SBI consists of a 30 cm aperture Dall-Kirkham telescope feeding a 320×240 element thermal detector array. The telescope primary and secondary mirrors are uncoated to reduce the irradiance to the level accepted by the detector. The detector is a barium strontium titanate (BST) thermal array modified by deposition of a thin coat of gold black to produce an essentially constant response to all wavelengths from the UV to beyond 10 μm in the IR.

The balloon-borne SBI provided the first images of the photosphere in evenly weighted, *broadband* light between about 0.31 μm (set by atmospheric transmission at balloon altitude) and 2.6 μm (set by quartz window absorption). This spectral interval contains approximately 94% of S . The SBI angular resolution of approximately 5" is adequate to separate spots, faculae, and the enhanced network from nonmagnetic cell interiors. The SBI provides measurements of broadband photometric *contrast* of localized structures, such as faculae, relative to their surroundings in the quiet photosphere. This measurement requires neither absolute calibration nor long-term reproducibility.

3. OBSERVATIONS

The SBI was launched from Fort Sumner, New Mexico, on 2003 September 1. Approximately 500,000 images were obtained during its 5 hr of data recording at an altitude of 33 km. The camera repetition rate was 30 Hz, and 60 frames were usually co-added to produce an image. Each image has a field of view of $917'' \times 687''$. Quick-look data suitable for checking the pointing and (auto-) focus algorithms were downlinked; most of the data were stored and recovered after return of the payload.

4. REDUCTION

Standard techniques for registering and co-adding images, flat-fielding and limb-darkening correction, were applied to the SBI images. A full disk mosaic before and after limb-darkening removal is shown in Figure 1. The photometric response of the SBI camera was determined in the laboratory to be linear to approximately $\pm 1\%$, up to the midrange of focal plane irra-

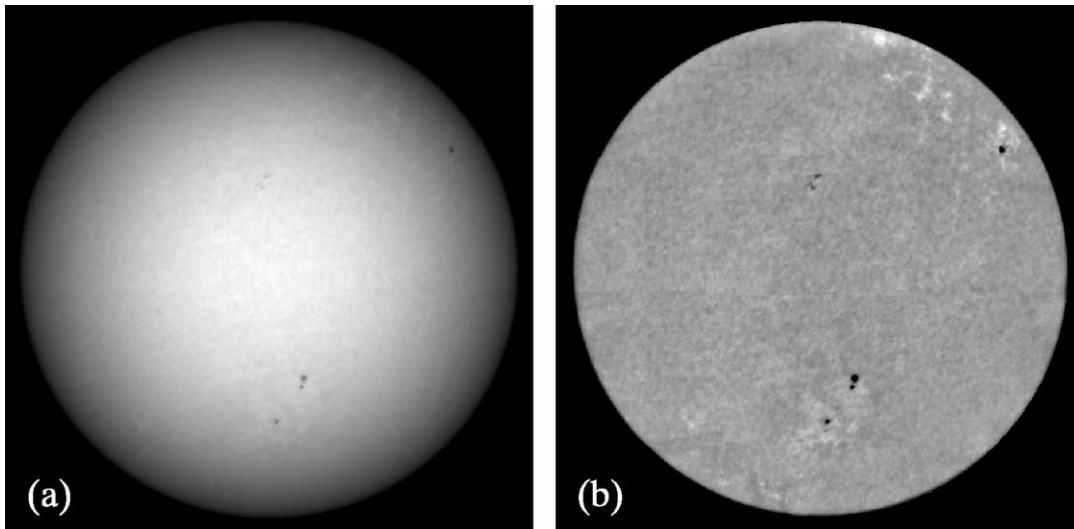


FIG. 1.—Full disk mosaic of SBI images on 2003 September 1 showing the photospheric disk before (panel *a*) and after (panel *b*) limb-darkening removal.

diance observed at balloon altitude. It becomes approximately 10% sublinear at the maximum of about 8500 counts recorded at disk center. This detector response is corrected during the data reduction process. Additionally, the response was checked with neutral density filters, first on the ground at Fort Sumner and then also at flight altitude. The scattered light in the SBI ground-based prototype was measured to be about 1% in visible light by measurements on the lunar limb (Foukal & Libonate 2001). Our observations at balloon altitude indicate a similar level in broadband light.

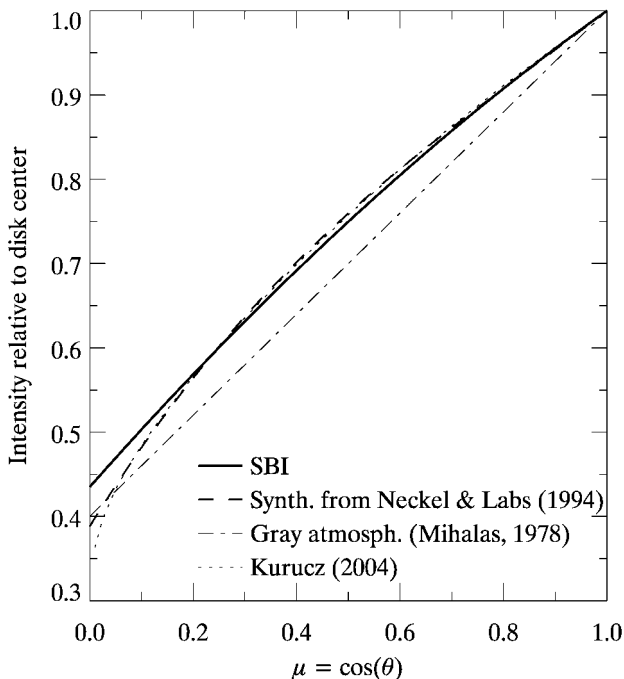


FIG. 2.—Photospheric limb darkening measured with the SBI (solid curve), synthesized from monochromatic data of Neckel & Labs (1994; dashed curve), a gray atmosphere model (e.g., Mihalas 1978; dot-dashed curve), and derived from a nongray LTE atmospheric model (R. L. Kurucz 2004, private communication; dotted curve).

5. RESULTS

5.1. Photospheric Limb Darkening

The SBI data provide the first opportunity to measure photospheric limb darkening in integrated light. Figure 2 shows the observed curve for comparison with (1) a curve we synthesized from limb darkening measured from the ground (Neckel & Labs 1994) and weighted by flux at these wavelengths; (2) a curve calculated from the standard formula for a gray atmosphere (e.g., Mihalas 1978); and (3) a theoretical curve calculated from a nongray LTE atmosphere (R. L. Kurucz 2004, private communication).

The SBI curve agrees to within $\pm 1\%$ with both the synthetic observational curve and the nongray LTE model, except nearer the limb than $\mu = 0.15$ (i.e., about $15''$). It lies systematically about 5% above the gray curve. The diagnostic value of this comparison for photospheric modeling is limited because the measured and calculated integrated-light curves combine contributions from a wider range of atmospheric depths than the more useful monochromatic curves. But the comparison does have two applications.

The increasing departure near the limb from the synthetic curve deserves attention. Future SBI measurements through a passband filter would enable us to examine this departure at specified wavelengths (e.g., Neckel & Labs 1994). A persistent difference in such measurements at a common wavelength would exclude solar effects.

Second, we note the systematic departure from the theoretical, gray limb-darkening curve. Gray limb darkening is used to derive the standard formula describing the relative weighting of spot and facular contributions to total irradiance, as a function of their limb distance (e.g., Willson et al. 1981). Our measurement indicates that the formula presently used underestimates the photospheric brightness relative to disk center by 5%–10%, so the contributions of spots and faculae to the irradiance away from disk center would tend to be underestimated.

5.2. Facular Photometric Contrast

Figure 3 shows intensity profiles taken through several faculae and one of the two small spots on the disk on 2003 Sep-

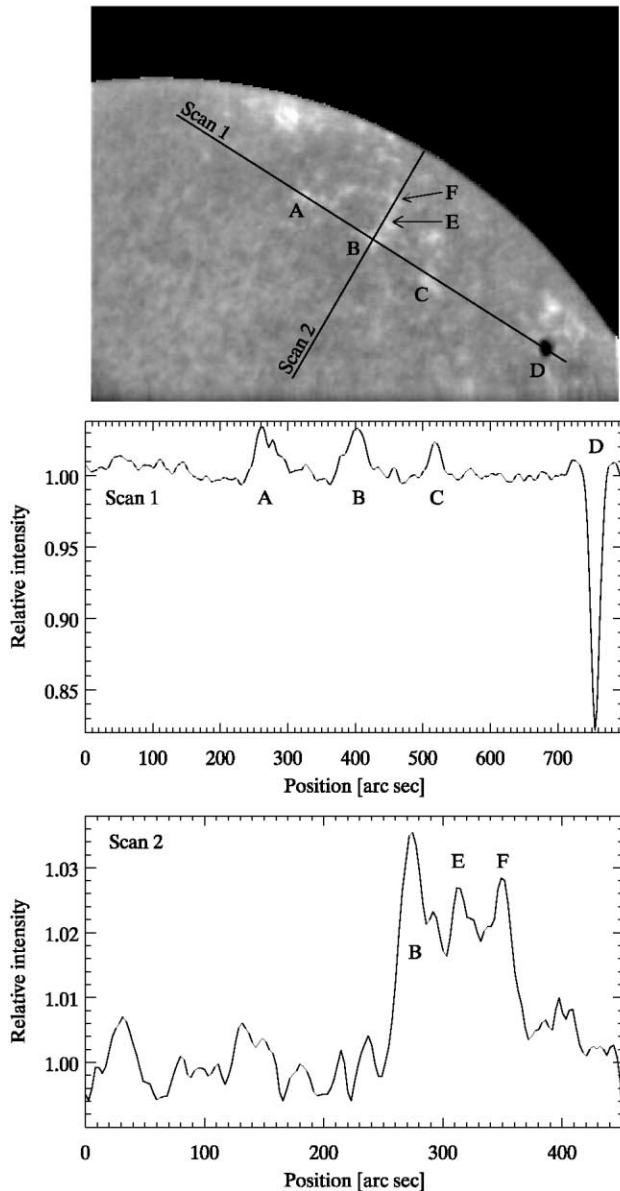


FIG. 3.—Illustration of the scan lines used to obtain some of the facular and sunspot contrast measurements. The region displayed lies on the west limb, i.e., in the upper right of the full disk mosaic shown in Fig. 1.

tember 1. These were obtained with a dwell time per pixel of only a few seconds, so granulation and p -mode noise have not yet been suppressed by co-adding the many such mosaics obtained during the flight.

The depth of the intensity depression for the spot (marked “D”) is about 17%. This contrast is significantly lower than obtained in ground-based observations with the SBI prototype on somewhat larger spots (Foukal & Libonate 2001), but it falls within the values measured for this same small spot during our flight with the Cartesian full disk telescope (CFDT) photometric scanner at the San Fernando Observatory, which has a similar ($\sim 5''$) angular resolution observing in three 10 nm passbands centered at 472, 672, and 780 nm.

The scans we show here through the SBI images show that the brightness of individual faculae such as the features marked A, B, C, E, and F is enhanced by about 3%–4%, and this can be measured against the background with a signal-to-noise ratio

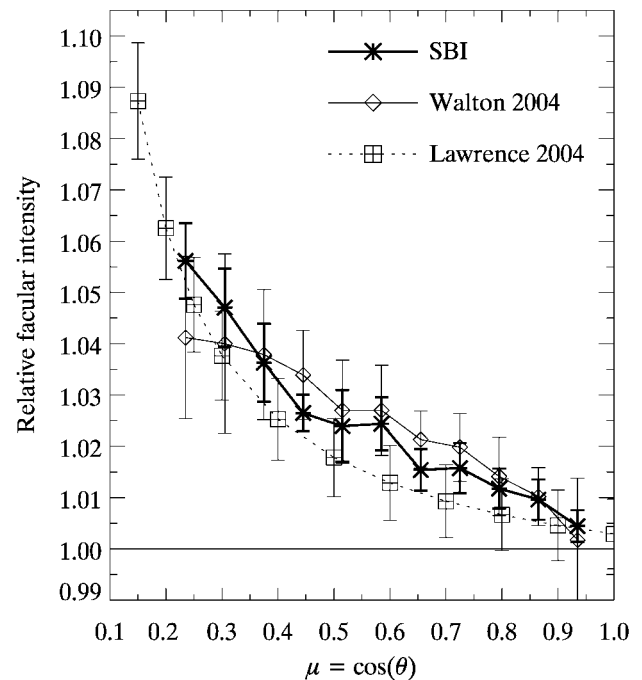


FIG. 4.—Curve of facular contrast, $I(f)/I(p)$, measured by SBI in integrated light, vs. $\mu = \cos(\theta)$ (asterisks). The vertical bars indicate the dispersion (1σ) of the SBI data. The squares show the bolometrically corrected monochromatic measurements of Lawrence (1988; J. K. Lawrence 2004, private communication). The diamonds show the equivalent red monochromatic measurements obtained at the San Fernando Observatory, of the same faculae measured by SBI on 2003 September 1.

of approximately 5 : 1 on individual scans of a single feature. Figure 4 shows the center-to-limb behavior of this enhancement when the observed faculae are binned by intervals of 0.07 in $\mu = \cos(\theta)$.

The faculae included in this plot have been selected by using a Ca K image obtained at the San Fernando Observatory during the SBI flight. This Ca K image was first corrected for limb darkening, and then a threshold was applied to choose structures whose contrast (in Ca K) exceeded their surroundings by a factor of 1.13. A mask was obtained from this thresholding, which was then applied to the SBI image.

The vertical bars in Figure 4 show the dispersion of the data. This is due in part to increased spatial smearing in the smaller faculae and in part to real intensity differences between individual faculae (e.g., Worden et al. 1998; Ortiz et al. 2002). The limited number of faculae on the disk in this flight accounts for the nonuniform sampling in $\mu = \cos(\theta)$. Presently, this limited sample size is probably the main source of uncertainty in our measurement since random error should be reduced to a few percent of the contrast value, by averaging over all the structures.

6. DISCUSSION

Our most interesting finding is the remarkable agreement between the SBI curve and a bolometric contrast curve shown in Figure 4, calculated (J. K. Lawrence 2004, private communication) using a simple blackbody correction to the monochromatic facular contrasts measured at a similar angular resolution by Lawrence et al. (1988). In this correction, the monochromatic contrast in a green (524.5 nm) or red (626.4 nm) passband of width 0.15 nm was used to calculate the blackbody temperature

from the Planck function. The temperature was then used to compute the broadband blackbody radiation at this temperature.

Also shown in Figure 4 is a similarly corrected curve supplied by S. Walton, based on monochromatic measurements at a comparable angular resolution, in a 10 nm passband at 672 nm, with the CFDT instrument at the San Fernando Observatory on the day of our balloon flight. The similarity in both amplitude and shape of these three curves supports the validity of a blackbody approximation to facular radiative excess, at least to the accuracy required for irradiance modeling. Similarly to the Lawrence et al. (1988) curve, the SBI contrasts fit well to a function in $1/\cos(\theta)$, namely,

$$C [\%] = (-0.75 \pm 0.03) + (1.57 \pm 0.09)/\cos(\theta).$$

7. CONCLUSIONS

The successful first balloon flight of the SBI demonstrates the solar photometric capabilities of this novel wideband imager. Our measurement of the photospheric limb darkening is the first in evenly weighted, integrated light, including over 94% of the total solar spectrum. Except very near the limb, it agrees within expected errors of about $\pm 1\%$ with a synthesis of narrowband limb-darkening curves and with a LTE nongray photospheric model. We suggest a test for the source of this difference, using future SBI observations through a narrowband filter.

Both of the *observational* curves of photospheric limb darkening in integrated light lie significantly (5%–10%) above the curve predicted by limb darkening in the gray approximation. This approximation has been widely used to weight the contributions of spots and faculae located at different limb distances in empirical modeling of the total solar irradiance. Incorporation of this small but systematic correction should improve the accuracy of such models.

The facular contrast curve we present here is the first to be measured in integrated light. Its agreement is remarkably good

in both amplitude and dependence on limb distance, with a curve obtained by a straightforward blackbody correction to a set of monochromatic measurements at similar angular resolution (Lawrence 1988; J. K. Lawrence 2004, private communication). The agreement suggests future use of such a simple correction to estimate facular contributions to total irradiance. This could be done a posteriori using existing monochromatic photometric imagery obtained regularly at, e.g., the San Fernando Observatory. Therefore, our SBI measurements make possible the relatively straightforward modification of existing irradiance models, which should soon enable us to make an accurate comparison in *amplitude* between the radiometric fluctuations and their photometric reconstruction, over the past two solar cycles.

The accuracy of our facular results is limited mainly by the relatively small sample of facular structures observed on 1 day of modest activity. A longer 2–3 week balloon flight, planned from Antarctica, would be desirable to improve this accuracy and to test the interesting result found here. SBI operation completely above the atmosphere would extend its spectral range into the more variable vacuum-ultraviolet spectral region estimated to account for 15%–20% of the total solar irradiance fluctuation (e.g., Fligge et al. 1998). Such space flight should include about 98% of the total solar irradiance, essentially the same fraction as is measured accurately by space-borne radiometers such as ACRIM and VIRGO (Variability of solar Irradiance and Gravity Oscillations).

We thank the JHU/APL engineering group and the NSBF staff at Fort Sumner, New Mexico, for their support. We are also grateful to Stephen Walton and John Harvey, to the HAO and Rome Observatory PSPT groups, and to the Stanford MDI group for providing us with excellent data in support of the SBI flight. We also thank Yvonne Unruh, Barry LaBonte, and Sami Solanki for comments on a draft of this Letter. This work was supported in part by NASA contract NAG5-10998 to JHU/APL and by NSF grant ATM 0303557 to Heliophysics, Inc.

REFERENCES

- Bernasconi, P. N., Eaton, H. A. C., Foukal, P., & Rust, D. M. 2004, *Adv. Space Res.*, 33, 1746
- Bernasconi, P. N., Foukal, P., Eaton, H. A. C., & Rust, D. M. 2003, AGU, Fall Meeting 2003, Abstract SH32A-1101
- Chapman, G. A., Cookson, A. M., & Dobias, J. J. 1996, *J. Geophys. Res.*, 101, 13541
- Fligge, M., Solanki, S. K., Unruh, Y. C., Frohlich, C., & Wehrli, Ch. 1998, *A&A*, 335, 709
- Foukal, P. 2003, *Eos*, 84, 205
- Foukal, P., Harvey, K., & Hill, F. 1991, *ApJ*, 383, L89
- Foukal, P., & Lean, J. 1986, *ApJ*, 302, 826
- . 1988, *ApJ*, 328, 347
- Foukal, P., & Libonate, S. 2001, *Appl. Opt.*, 40, 1138
- Krivova, N., Solanki, S., Fligge, M., & Unruh, Y. 2003, *A&A*, 399, L1
- Lawrence, J. K. 1988, *Sol. Phys.*, 116, 17
- Lawrence, J. K., Chapman, G. A., & Herzog, A. D. 1988, *ApJ*, 324, 1184
- Lawrence, J. K., Topka, K. P., & Jones, H. P. 1993, *J. Geophys. Res.*, 98, 18911
- Lean, J., Cook, J., Marquette, W., & Johansson, A. 1998, *ApJ*, 492, 390
- Mihalas, D. 1978, *Stellar Atmospheres* (2nd ed.; San Francisco: Freeman)
- Neckel, H., & Labs, D. 1994, *Sol. Phys.*, 153, 91
- Ortiz, A., Solanki, S., Domingo, V., Fligge, M., & Sanahuja, B. 2002, *A&A*, 388, 1036
- Willson, R. C., Gulkis, S., Janssen, M., Hudson, H. S., & Chapman, G. A. 1981, *Science*, 211, 700
- Worden, S., White, O., & Woods, T. 1998, *ApJ*, 496, 998